Physical Interpretations of the Numerical Instabilities in Diffusion Equations Via Statistical Thermodynamics

M. Bigerelle and A. Iost

Laboratoire de Métallurgie Physique et Génie des Matériaux (UST Lille),

Equipe Surfaces et Interfaces (ENSAM Lille) - CNRS UMR 8517.

ENSAM Lille, 8 boulevard Louis XIV, 59046 LILLE Cedex, FRANCE

Abstract

The aim of this paper is to analyze the physical meaning of the numerical instabilities of the parabolic partial differential equations when solved by finite differences. Even though the explicit scheme used to solve the equations is physically well posed, mathematical instabilities can occur as a consequence of the iteration errors if the discretisation space and the discretisation time satisfy the stability criterion. To analyze the physical meaning of these instabilities, the system is divided in sub-systems on which a Brownian motion takes place. The Brownian motion has on average some mathematical properties that can be analytically solved using a simple diffusion equation. Thanks to this mesoscopic discretisation, we could prove that for each half sub-cell the equality stability criterion corresponds to an inversion of the particle flux and a decrease in the cell entropy in keeping with time as criterion increases. As a consequence, all stability criteria defined in literature can be used to define a physical continuous 'time–length' frontier on which mesoscopic and microscopic models join.

Keywords: Diffusion, Partial Differential Equations, Finite Difference Method, Stability, Fractal, Monte Carlo, Entropy, Anti Entropy Process, Brownian Motion.

1 Introduction

The rapid development of high-speed computer technology over the recent years has been accompanied by a very substantial growth of computational science. A high number of physical phenomena can be modeled by Partial Differential Equations (PDE) [1] that can be solved by numerous numerical methods [2-3]. Among these methods, only the Finite Difference Method (FDM) [4], which stands out as being universally appropriate to both linear and non-linear problems, is considered here. FDM can equally be applied to hyperbolic, elliptic and parabolic equations. In short, these equations are used to model wave physical properties, time-stationary phenomena and all time dependent diffusion (transport) processes. To solve these PDE numerically, FDM consists in expanding all variables of the PDE in Taylor series on a grid at different points in the relevant domain, while limiting this expansion to the first derivatives, introducing these finite expansions on the PDE problem and finally solving it by adequate numerical models. The main problem encountered is that PDE becomes a discretised equation in which all differential elements do not tend towards zero but towards fixed values that depend on the number of discretised points. However, the discretisation process involves local truncation errors and the problem of the consistency of the numerical scheme is raised, i.e. the solution converges towards the solution of PDE as the mesh length tends towards zero. Supposing that the numerical scheme is consistent, a second problem consists in testing the stability of this scheme since all rounding errors introduced during computation (as a

consequence of the finite representation numbers) increase during the iterative scheme itself that may become unstable. Many mathematical tools and theorems can be used to study the stability of the system. However no physical interpretation has been proposed yet. These methods show that by increasing the discretisation time, the system may pass from stability to instability. In fact, these mathematical results involve questions about the physical modeling process. There exists a space-time relation that allows us to solve the problem of consistence related to Chaos Theory: a small initial error may be raised and become very important leading to a total instability of the system [5]. However PDE model macro physical systems and the fundamental questions are: 'Is the length of the space-time unit used in discretisation compatible with the microscopic phenomena? If not does it lead to an unstable system?' With regard to the high number of mathematical publications related to PDE stability, we propose to study physically the stability of a parabolic PDE that can be applied onto physical problems which are easily modeled at the microscopic scale.

In a first part of the present paper, we shall describe the physical use of these equations. Secondly, we shall analyze the numerical solution of the well-known Fick equation [6] compared with the Einstein model [7] to find out if the problem is well posed. In a third part, we shall introduce briefly a new method for studying stability. In a fourth part, we shall propose a physical interpretation of stability based on Brownian motion theories [5,7] and the second principle of thermodynamics [8]. Finally we shall proceed a Monte Carlo simulation to illustrate our physical stability interpretation.

2 Parabolic Differential Equations

The Parabolic PDE is given by the following mathematical definition:

$$\frac{\partial u}{\partial t} - \sum_{i,j}^{n} \frac{\partial}{\partial x_i} a_{i,j} \frac{\partial}{\partial x_j} u - f(x,t) \qquad (1)$$

where $(x,t) \in \Omega \times \mathbb{R}_+$, and Ω is an open set of $\mathbb{R}^n$.

These equations that characterize transport phenomena such as heat transfer, viscous fluid mechanics, atom-vacancy transport, Ohm law, contagious epidemic ... can be obtained by three main ways:

(1) Counting the number of "particles" by volume unit and applying a Fick law flux $J \propto grad(u)$;

(2) Using transport equations for each entity of the system (particle) and making the free path tend towards zero;

(3) Using stochastic processes as Brownian motion.

These mathematical methods, used for physical modeling, show that the diffusion process can be derived from probabilistic topics, meaning that diffusion laws are stochastic in nature. Asymptotic considerations will lead to suppressing the stochastic aspect of these models to obtain deterministic ones. In other terms, microscopic fluctuations are "removed" to result in macroscopic formulations, i.e. continuous ones. One important consequence of this fundamental duality is that the differential elements can not have a zero limit that would lead to a nonsensical interpretation. For example, in the Fourier heat transfer law, heat can be considered as the Brownian motions of phonons/electrons and then the differential elements cannot be smaller than the mean free path of the motion. On the contrary, the differential elements must not be too large to include the mesoscopic modeling of the phenomenon. These considerations show that there exists a scale range where the differential elements get a physical meaning, whose determination is no trivial work.

3. The resolution of the diffusion equation

3.1. Analytical solution

Equation 1 can be analytically solved for only specific systems, and therefore a numerical estimation has to be generally processed. In this part Eq.1 is discretised by the Finite Difference Method. Without lack of generality, we shall retain to treat in this paper the simple mono-

dimensional Fick equation that is reduced to:

$$\frac{\partial C(x,t)}{\partial t} = D \frac{\partial^2 C(x,t)}{\partial x^2}, \qquad (2)$$

where $C(x,t)$ is the concentration at time t of particles at position x, and D the diffusion coefficient. With $C(0,0) = C_0 \delta_0$, where δ_0 is the Dirac pulse, and   as initial conditions, the well-known solution is:

$$C(x,t) = \frac{C_0}{2\sqrt{\pi D t}} \exp\left(-\frac{x^2}{4Dt}\right). \qquad (3)$$

We shall precise some of its properties. Firstly, Eq.3 reduced by C_0 is a Gaussian Probability Density Function (PDF) with zero mean and $\sigma(t) = \sqrt{2Dt}$ standard deviation. This clearly means that diffusion is a stochastic process and that equations can be obtained by asymptotic considerations (like the Central Limit Theorem). To visualize this fact, a Monte Carlo method will be used in chapter 5 to simulate the diffusion process on purpose to compare with the theoretical solution given by Eq.3.

3.2. Numerical solution

We shall now use the finite difference method to discretise Eq.2. Using Taylor expansions:

$$\left.\frac{\partial C(x,t)}{\partial t}\right|_{x=i\Delta x, t=j\Delta t} \approx \frac{C(i\Delta x, (j+1)\Delta t) - C(i\Delta x, j\Delta t)}{\Delta t}$$

$$+\Theta(\Delta t) = \frac{C_i^{j+1} - C_i^j}{\Delta t} + \Theta(\Delta t),$$

and

$$\left.\frac{\partial^2 C(x,t)}{\partial x^2}\right|_{x=i\Delta x, t=j\Delta t} \approx \frac{C_{i-1}^j - 2C_i^j + C_{i+1}^j}{(\Delta x)^2} + \Theta\left((\Delta x)^2\right) \quad ,$$

which gives the following explicit numerical scheme:

$$C_i^{j+1} = C_i^j + \frac{D\Delta t}{(\Delta x)^2}\left(C_{i-1}^j - 2C_i^j + C_{i+1}^j\right). \qquad (4)$$

On the other hand, if the gradient is considered at time $t = (j+1)\Delta t$, then the following implicit numerical scheme is obtained:

$$\left.\frac{\partial C(x,t)}{\partial t}\right|_{x=i\Delta x, t=j\Delta t} \approx D \left.\frac{\partial^2 C(x,t)}{\partial x^2}\right|_{x=i\Delta x, t=(j+1)\Delta t} ,$$

$$C_i^{j+1} = C_i^j + \frac{D\Delta t}{(\Delta x)^2}\left(C_{i-1}^{j+1} - 2C_i^{j+1} + C_{i+1}^{j+1}\right). \qquad (5)$$

Or more generally:

$$C_i^{j+1} = C_i^j + \frac{D\Delta t}{(\Delta x)^2}\left[\begin{array}{l}\beta\left(C_{i-1}^j - 2C_i^j + C_{i+1}^j\right) + \\ (1-\beta)\left(C_{i-1}^{j+1} - 2C_i^{j+1} + C_{i+1}^{j+1}\right)\end{array}\right], \qquad (6)$$

which corresponds to the well-known Crank-Nicholson scheme for $\beta - 0.5$.

Equation 4 is an explicit scheme meaning that concentration at time $t + \Delta t$ only depends on the gradient at time t. Equation 5 is an implicit scheme meaning that concentration at time $t + \Delta t$ only depends on the gradient at time $t + \Delta t$. Neglecting problems of discretisation errors (which will be minimized when $\beta = 0.5$ in Eq.6.) and numerical stability, the question which arises from our analysis is to know whether the scheme gets a physical sense or not.

3.3. The implicit/explicit scheme and the Einstein theory of Brownian motion

To answer the above question, we shall analyze the hypothesis used by Einstein in 1905 to give a physical explanation to the phenomenological coefficient D in Eq.2 introduced by Fick. Einstein postulated that concentration at time $t + \Delta t$ is given by:

$$C(x, t+\Delta t) = \sum_{i \in p} W(X_i, \Delta t) C(x - X_i, t), \qquad (7)$$

where $W(X, \Delta t)$ is the probability that an i particle makes a X_i long jump during a time Δt. This equation is reduced to Eq.2 by posing $D = \lim_{\Delta t \to 1}\left(\langle X^2 \rangle / 2\Delta t\right)$. As a consequence, Einstein shows that the particle concentration at time $t + \Delta t$ only depends on average on the concentration at time t, i.e. before the jump occurs. The implicit scheme ($\beta = 0$) lets us suppose an instantaneous jump, which is a physical non-sense.

The main criticism against the implicit scheme is that we cannot affirm that all particles would jump simultaneously at time t, which is in fact well founded. However this problem is still under discussion: in a discretised space, the mesoscopic time Δt ($\Delta t \gg \Gamma^{-1}$ where Γ is the atom jump frequency) could be used without any physical problem to model the diffusion states without taking into account the correlation effects, and then the particles can jump

simultaneously. However, even if time is mesoscopic, Eq.7 can be transformed into:

$$C(x, t + \Delta t) = \sum_{i \in p} W(X_i, \Delta t - \Delta t_i) C(x - X_i, t - \Delta t_i), (8)$$

and Δt_i ($\Delta t_i \ll \Delta t$) will be seen as time fluctuation. By introducing this perturbation in the probability jump, the variance properties of the concentration become less smooth than the average solution. This result was reported by El Naschie in his study of the abnormal diffusion and correlation in the Cantorian space [9]. The fractal space-time cannot exactly be d=2, but must be slightly larger because diffusion on a lattice and in a random environment is harder than in a smooth space. Therefore the fractal dimension must be taken as the mean $<d_c> = 2$ rather than $d_c = 2$. As a consequence, introducing a perturbation in the Einstein diffusion equation will not affect the solution on average, like the mesoscopic diffusion problems in the EDP theory. However the Fractal concepts of the Brownian motion show that the positions of the particles $X(t)$ possess the property $\langle (X(t + \Delta t) - X(t))^2 \rangle \propto \Delta t$ and the graph $X(t)$ versus time possesses a statistical self-affine structure meaning that

$$\langle X(t + \Delta t) - X(t) \rangle = r^{-0.5} \langle (X(t + r\Delta t) - X(t)) \rangle$$ As a consequence, time and distance do not possess a Euclidean metric and then to use a Euclidean formulation (integer integration of PDE), as used by Einstein, the Brownian Motion must be located at a constant time Δt involving a constant displacement X. Therefore, in the average dimension analysis, the formulation of Eq.8 is rejected for Einstein's Eq.7. All these remarks show that only the explicit formulation gets a physical meaning even though Eqs.(5-6) introduce some physical non-sense.

4. Stability study

4.1. The stability-instability transition

We have shown that the explicit scheme gets a physical sense that the implicit one does not possess. As concentration at time $t + \Delta t$ is calculated from concentration at time t, the explicit scheme becomes a dynamic system given by Eq.5 that may become unstable for a
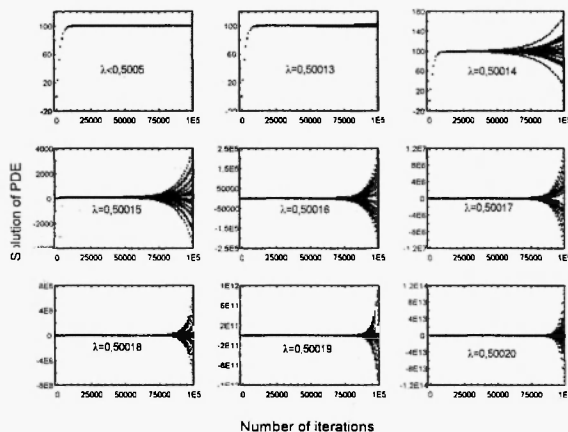

Fig. 1. Numerical estimation of a PDE problem in the middle of the grid $C_\lambda(50, t)$ versus the number of iterations used in the numerical scheme for different values of the stability criterion λ. 20 simulations are computed with different initial noises. The analytical solutions are $\lim_{t \to \infty} C(50, t) = 100$.

given set of values $D\Delta t / (\Delta x)^2$. The essential idea behind stability is that a numerical process, when applied wisely, should limit the amplification of all components of the initial conditions including rounding errors. The basic analysis considers the growth of perturbations in initial data or the growth of errors introduced at mesh points at a given time level. To us, this mathematical philosophy seems close to the Chaos Theory philosophy and as a consequence we postulate that a duality exists between the mathematical interpretation and the physical representation. Three common methods exist to investigate stability: the Von Neumann method, the matrix method, and the energy method [4]. Using one of these three methods, it can be shown [4] that the explicit scheme will be stable if:

$$\lambda = \frac{D\Delta t}{(\Delta x)^2} \leq \frac{1}{2}. \tag{10}$$

A stochastic simulation will be used to illustrate the PDE stability. Let us take the following parameters to process the numerical simulation: $D=1$, $\Delta x = 1$, $C(0, t) = 100$, $C(100, t) = 100$ and $C(x, 0) = U, x \in \{1...99\}$ where U is a random value that follows a uniform law in the range

$U \in [-0.5 \cdots 0.5]$ used to introduce a perturbation in the numerical scheme. The analytical solution gives $\lim_{t \to \infty} C(x,t) = 100$, $\forall x$. Then the explicit scheme is used to calculate the values of $C_\lambda(x,t)$ at different times and space discretised points. For sufficiently large values of t ($t = t_\infty = 100000$) we can admit that the solution is reached since convergence errors are lower than computer errors due to finite representation numbers. To analyze stability, we shall compute the estimation values $C_\lambda(50,t)$, the concentration in the middle of the medium at different times for different values of λ ($\lambda \in [0.40000, 0.50020]$). Fig.1 is the plot of $C_\lambda(50,t)$ versus time for different values of λ (for a given λ, 20 simulations are computed with different initial noises U). For $\lambda < 0.5005$, the initial noise decreases during iterations and the numerical solution $C_\lambda(50,t)$ converges towards the true value i.e. 100. This threshold is slightly higher than the 0.5 theoretical value, which is not in contradiction with the stability theory. In fact, this theory affirms only that a numerical scheme will be unconditionally stable for $\lambda < 0.5$, i.e. whatever the initial conditions, the frontier conditions, Δt , Δx or D , the scheme will always be stable if $\lambda \leq 0.5$. The theory does not affirm that some particular conditions can lead to stability for $\lambda_c > \lambda > 0.5$. For example, with $\Delta x = 10$, $\lambda_c = 0.512$ and $\Delta x = 5$ leads to $\lambda_c = 0.503$ (in fact, we have shown that if all parameters stay unchanged, $\lim_{\Delta x \to 0} \lambda_c = 0.5$). Fig.1 shows that for $\lambda > 0.5005$, a noise appears on the values $C_\lambda(50,t) = 100$ that will be exponentially amplified with an increase of λ : the scheme becomes unstable. Then, we estimate the error by:

$$Er(x/2,t_\infty) = \log |C_\lambda(x/2,t_\infty) - 100|^2 .$$

Fig.2 represents this error function versus λ and confirms that after $\lambda \geq 0.50005$, error increases exponentially according to the power-law:

$$|C_\lambda(x/2,t_\infty) - 100|^2 \propto \lambda^{3.6 \, 10^5} .$$

4.2. Space-time dimension and stability process

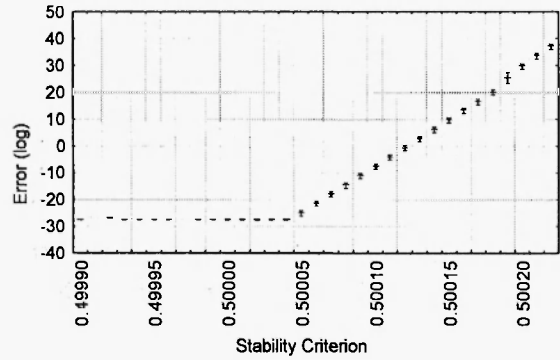Before giving a physical interpretation, five

Fig. 2. Numerical estimation of the error for a PDE problem in the middle of the grid $C_\lambda(50,t)$ versus the number of the iterations used in the numerical scheme for different values of the stability criterion λ. 20 simulations are computed with different initial noises and means on $C_\lambda(50,t)$. The associated 95% confidence levels are plotted.

remarks about inequality (10) have to be made:
1) For given values of D and Δt , if the space increment Δx decreases, then after a critical value, the scheme becomes unstable. In other words, the time Δt is too large to isolate the diffusion phenomenon on a length Δx . In the same way, if Δt decreases Δx must decrease, i.e. the length must be small enough to isolate the diffusion flux during Δt time which looks like a kind of macroscopic uncertainty principle.
2) Since diffusion can be seen as a random process $X(t)$ with Gaussian increment we obtain:

$$\text{var}[X(t_2) - X(t_1)] \propto |t_2 - t_1|^{4-2D_f} , \qquad (11)$$

where $D_f = 1.5$ is the average fractal dimension of the Brownian motion graph and var(X) the variance of X. A characteristic length Δx of the displacement can be given by the standard deviation of Eq.11 and then $\sqrt{\text{var}[X(t_2) - X(t_1)]} = \Delta x$. Therefore $\Delta t = |t_2 - t_1|$ can be seen as the characteristic length associated with Δt time and we obtain $\Delta x \propto \sqrt{\Delta t}$ or $\Delta t/(\Delta x)^2 = cte$ that represents a limit condition between stability and instability. As a consequence, the criterion of stability follows the same relation as the relation between time and distance in the fractal concept of diffusion.

```
                STABLE        |           UNSTABLE

Macroscopic                   |          no interaction particle
System _____ ⊥ _____ ⊥ _____
                              | Velocity         |
                              | and interaction  |
                              | particles    ⎡ Dc = πm/h ⎤
Particle _____ ⊥ _____ ⊥ _____
                              1                  h
                             2D                 2πm
                        MEASURABLE         |    UNMEASURABLE

| ----------------------------------------------------------→   Δt
                                                              ─────
                                                              (Δx)²
```
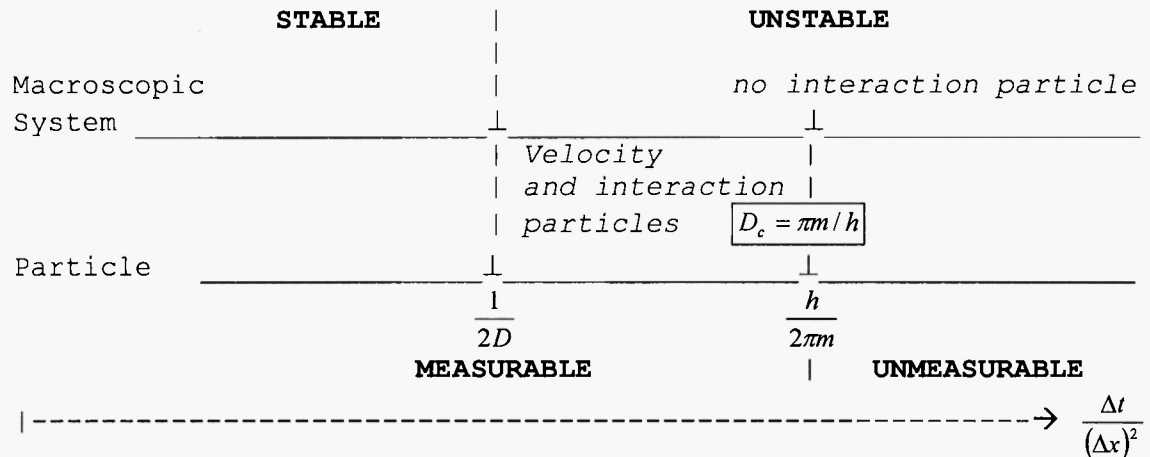
Table 1

Another stability criterion (with different power exponents) will be incompatible with the space-time relation for the fractal motion of a particle.

3) Let us analyze the solution of a sandwich of particles that diffuse in an infinite medium. The solution is given by Eq.3. This solution is a Gaussian PDF (at a constant factor) with a zero mean and a $\sigma(t) = \sqrt{2Dt}$ standard deviation. According to the properties of the Gaussian PDF, 66% of the diffused mass are in the interval $[-\sigma(t), \sigma(t)]$, 95% in $[-2\sigma(t), 2\sigma(t)]$, 99.7% in $[-3\sigma(t), 3\sigma(t)]$ ... This clearly means that the value $\Psi(P)\sigma(t)$ with:

$$\int_{-\Psi(P)}^{\Psi(P)} \frac{1}{\sqrt{2\pi}} \exp\left(-\frac{x^2}{2}\right) dx = P \ , \qquad (12)$$

can be seen as a mean diffusion front (without any fractal aspect) and as a consequence $L(P) = \Psi(P)\sqrt{2Dt}$ becomes a characteristic length of the diffusion progression. Considering now each discretised space length Δx , an elementary sandwich diffusion process centered on Δx interval must statistically keep a certain mass on the Δx interval, then $\Psi(P)\sqrt{2Dt} < \Delta x$ and finally:

$$\frac{D\Delta t}{(\Delta x)^2} = \frac{\Psi(P)}{2} \ . \qquad (13)$$

This condition looks like the stability condition given by Eq.10. It physically means that stability can be obtained in a macroscopic system only if the adimensional parameter $D\Delta t/(\Delta x)^2$ is lower than a characteristic length related to the diffusion process. It must be emphasized that the main relation of the thermodynamic interpretation of this instability proposed in the following paragraph exactly leads to the stability conditions of the EDP when posing $\Psi(P)=1$, as a result of the Gaussian properties related to the inflexion point.

4) From the Heisenberg principle, $\Delta x\Delta p \geq \hbar$ and then $\Delta t/\Delta x^2 < h/2\pi m$. This relation looks like a stability criterion. As $1/2D < 1/2D_c = h/2\pi m$ (meaning that $D \geq D_c = \pi m/h$), D_c is the smallest Diffusion Coefficient (without any environmental interactions) that can be measured according to the uncertainty principle and which leads to a stable scheme.

If $\Delta t/(\Delta x)^2 \in [1/2D, h/2\pi m,]$ (see table 1) then the scheme is unstable but the particle flux can be measured. D is a macroscopic coefficient that represents the easiness with which a number of atoms passes through a fictive interface by time unit. This means that D involves a correlation effect, interactions between atoms, a potential barrier not involved in D_c (Heisenberg Principle concerns isolated particles). In the range $[D, D_c]$, all is seen if measurable instability is due to the interaction between particles, velocity ... which seems to converge to the fact that chaos will appear when different systems interact and these interactions are related to the coefficient D.

5) If D increases for a constant value of $\Delta t/(\Delta x)^2$ (constant space-time observation), the system might become unstable. Increasing D corresponds to increasing the diffusion front

length in the elementary cell and then from (13) the system may become unstable. With a same value of space-time observation, the map might become unstable when the velocity of the particle increases (e.g. increasing temperature increases D) which is a well-known expression of the emergence of chaos in the fluid as observed in the classical Taylor-Couette experimentation [10].

5. Physical interpretation of stability

We shall now introduce a physical interpretation of stability in which we suppose that Eq.2 governs the diffusive system. This equation can be seen as modeling the diffusion in all the media and therefore is an intrinsic physical property of the system. In this system, we shall introduce the initial concentration $C(x,0)$, a space description Ω (open set of IR), and limit conditions $C(\mathbf{x},t)$ (or another condition like the flux condition $\partial C(\mathbf{x},t)/dx$ ... where $\mathbf{x} \in \partial\Omega$). The important fact is that these conditions do not change the physics of the diffusion but only give a particular configuration to the system. As there can be an infinite number of initial or limit conditions, the number of solutions for the differential system becomes infinite and generally cannot be solved analytically. All solutions can be seen as density functions because concentration in space dx can be seen as a probability to find particles in dx. In this part, we shall prove that all time-diffusion systems can be seen as the sum of elementary sandwich processes centered on each part of a grid equally spaced.

5.1 Relation between stochastic microscopic diffusion state and microscopic deterministic diffusion state

Let us consider the diffusive system as a microscopic one and note n the number of particles at time t at position $x_i(t)$, $i \in \{1...n\}$. As the position cannot be known exactly (Heisenberg's principle), we can consider that the probability to find a particle is given by:

$$\varphi(x_i,t;h) = \frac{1}{h\sqrt{2\pi}}\exp\left(-\frac{1}{2}\left(\frac{x(t)-x_i(t)}{h}\right)^2\right), \quad (14)$$

where h represents the lack of precision in the $x_i(t)$ determination (if $h \to 0$, then $\varphi(x_i,t;h) \to \delta_{x_i(t)}$, and the position is perfectly known). We shall now link the microscopic interpretation to the macroscopic system. Let us note $C(x,t)$ the solution of the PDE problem and $C(x,t,n)$ the solution given by the microscopic one. As a consequence, using the Gaussian Kernel Density Estimate we get:

$$C(x,t,n;h) = \frac{1}{nh}\sum_{i=1}^{n}\varphi(x_i,t;h). \quad (15)$$

The constant h is chosen to fit well with the macroscopic concentration that can be explained by a L^2 norm minimization:

$$\min_{h \in IR}\|C(x,t,n;h)-C(x,t)\|^2. \quad (16)$$

It can be shown that:

$$\lim_{n\to\infty}\min_{h \in IR}\|C(x,t,n;h)-C(x,t)\|^2 = 0 \text{ for } h \to 0.$$
$$(17)$$

meaning that a stochastic microscopic system tends towards a macroscopic deterministic one when the number of particles tends towards infinity.

5.2. Decomposition of complex macroscopic diffusion systems into elementary mesoscopic diffusion microstates.

Let us now suppose that the concentration $C(x,t)$ is known (for example Fig. 3(b_1) or Fig. 3(b_5). We discretise space in intervals of length Δx. On each interval labeled by n suffix, the concentration is a constant modeled by a rectangular function $H(x_n, \Delta x)$ (see Fig. 3(a1)) so that the concentration $C_n(x,t,\Delta x)$ on the central interval x_n is given by (for example Fig. 3(a1) or Fig. 3(a5)):

$$C_n(x,t,\Delta x) = C(x_n,t)H(x_n,\Delta x). \quad (18)$$

Then the discretised concentration $C(x,t,\Delta x)$ is given by:

$$C(x,t,\Delta x) = \sum_{n,n} C_i(x,t,\Delta x). \quad (19)$$

On each interval, the diffusion governed by Eq.2 still occurs, but with the initial condition on

these intervals given by:

$$\begin{cases} C_n(x,t,\Delta x) = C(x_n,t,\Delta x) \\ C_n(x,t,\Delta x) = 0 \end{cases},$$

$$\forall x \in [x_n - \Delta x/2, x_n + \Delta x/2]$$
$$\forall x \notin [x_n - \Delta x/2, x_n + \Delta x/2] \qquad (20)$$

When interval t is discretised in the time interval $[t, t + \Delta t]$, labeled by m suffix ($[t_m, t_m + \Delta t] = [t_m, t_{m+1}]$), we obtain:

$$\begin{cases} C_{n,m}(x,t_m,\Delta x) = C(x_n,t_m,\Delta x) \\ C_{n,m}(x,t_m,\Delta x) = 0 \end{cases},$$

$$\forall x \in [x_n - \Delta x/2, x_n + \Delta x/2]$$
$$\forall x \notin [x_n - \Delta x/2, x_n + \Delta x/2], t = [t_m, t_m + \Delta t]. \quad (21)$$

This means that the initial PDE problem can be modeled by a great number of cells on which the initial concentration is constant where Eq.2 holds.

The solution to Eq.2 on this "PDE-cell" is then given by:

$$C_{n,m}(x,t,\Delta x) = \frac{C(x_n,t_m,\Delta x)}{\sqrt{4\pi D(t-t_m)}} \int_{-\Delta x/2}^{\Delta x/2} \exp\left(-\frac{(x-x_n)^2}{4D(t-t_m)}\right) dx$$

$$(22)$$

After integration of Eq.22, the final solution is:

$$C_{n,m}(x,t,\Delta x) = \frac{1}{2} C(x_n,t_m,\Delta x) \left[\begin{array}{c} erf\left(\dfrac{\Delta x/2 - (x-x_n)}{\sqrt{4D(t-t_m)}}\right) + \\ erf\left(\dfrac{\Delta x/2 + (x-x_n)}{\sqrt{4D(t-t_m)}}\right) \end{array} \right]$$

$$(23)$$

with $erf(x)$, the error function given by

$$erf(x) = \frac{2}{\sqrt{\pi}} \int_0^x \exp(-u^2)\, du.$$

Theorem 1:

$$\lim_{t \to \infty} C_{n,m}(x,t,\Delta x) = \frac{C(x_n,t_m,\Delta x)}{\sqrt{4\pi D(t-t_m)}} \exp\left(-\frac{(x-x_n)^2}{4Dt}\right).$$

$$(24)$$

This means that for a long enough diffusion time, the PDE-cell is physically equivalent to the well-known problem of sandwich diffusion centered on the x_n value. The convergence rate of theorem 1 will be analyzed in the next chapter.

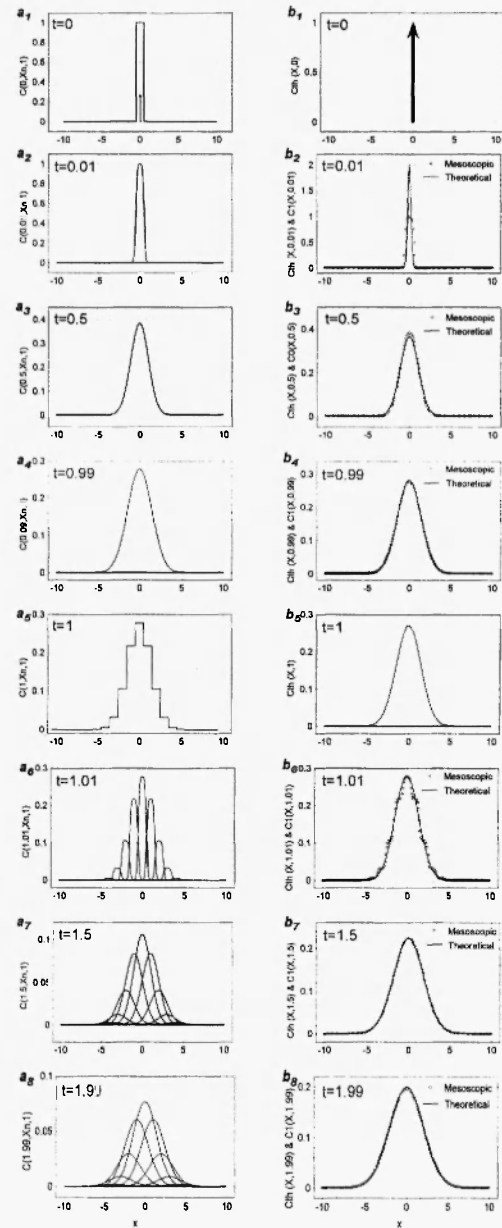Theorem 2: The solutions $C(x,t)$ to all the

Fig. 3. Evaluation of a diffusion problem for a thin material diffusing in a random medium. Values of $C(x_n, t_m, \Delta x)$ for different diffusion times are plotted on Fig.(a_1) to Fig.(a_8). Fig.(a_1) ($t = t_0 = 0$) and Fig.(a_5) ($t = t_1 = 1$) are calculated by integration of theoretical values $C_{th}(x,0) = \delta_0$ (Fig.(a_1)) and $C_{th}(x,1)$ (Fig.(a_5)). Fig. (b_2), (b_3), (b_4), (b_6), (b_7), (b_8) represent the sum of $C(x_n, t_m, \Delta x)$, i.e. $C_m(x,t)$, given on the left figure (circle). The theoretical values given by the PDE problems are plotted on filled line.

diffusion problems in infinite media (or where concentration in all the media does not change) which obey Eq.2, are solved by Eq.23 on each PDE-cell and then the macroscopic solution is given by:

$$C(x,t) = \lim_{\Delta x \to 0} \sum_{n \in N} \frac{C(x_n, t_0, \Delta x)}{\sqrt{4\pi Dt}} \int_{-\Delta x/2}^{\Delta x/2} \exp\left(-\frac{(x-x_n)^2}{4Dt}\right) dx$$

(25)

where $C(x_n, t_0, \Delta x)$ is the initial concentration in each cell.

To illustrate this theorem that is the central point of our physical approach to stability, we shall treat the macroscopic problem of initial thin film that diffuses in an infinite matrix. Eq.3 gives the solution to the macroscopic diffusion problem. The method described below is then applied with the following parameters:

$D = 0.01$, $\Delta x = 1$, $t \in [0...2]$, $t_m \in \{0,1\}$.
$n = \{-10, -9, ..., 9, 10\}$.

At each time where $t = t_m$, the values of $C(x_n, t_m, \Delta x)$ have to be numerically assessed. We calculate the mean of the concentration $\overline{C}(x_n, t_m, \Delta x)$ on the interval $[x_n - \Delta x/2, x_n + \Delta x/2]$ given by:

$$\overline{C}(x_n, t_m, \Delta x) = \frac{1}{\Delta x \sqrt{4\pi Dt_n}} \int_{-\Delta x/2}^{\Delta x/2} \exp\left(-\frac{(x-x_n)^2}{4Dt_m}\right) dx.$$

(26)

and then from Eq.18

$C(x_n, t_m, \Delta x) = \overline{C}(x_n, t_m, \Delta x) H(x_n, \Delta x)$ (for $t_m = 0$,
$C(x_0, t) = \delta_0$, Fig 3 (b_1) and
$C(x_n, t_0, \Delta x) = H(x_n, \Delta x)/\Delta x$, Fig. 3 (a_1)). Then Eq.23 is applied to calculate the concentration on each cell at different times $C_{nm}(x, t, \Delta x)$. Fig. 3.(a). represents the different values of $C_{nm}(x, t, \Delta x)$ for $m = 0$ (Fig.3 (a_1). to Fig.3 (a_4)) and $m = 1$ (Fig.3 (a_5) to Fig.3 (a_8)). To verify the correspondence with the theoretical value (3), we calculate the concentration obtained by our "Mesoscopic" model from theorem 2:

$$C_m(x,t) = \sum_n \frac{C(x_n, t_m, \Delta x)}{\sqrt{4\pi D(t - t_m)}} \int_{-\Delta x/2}^{\Delta x/2} \exp\left(-\frac{(x-x_n)^2}{4D(t - t_m)}\right) dx$$

(27)

and then compare with the theoretical values $C_{th}(x,t)$ given by Eq.3. Fig.3 (b_1) to Fig.3 (b_8) represent $C_m(x,t)$ and $C_{th}(x,t)$ for different diffusion times. As can be observed, the mesoscopic problem converges towards the analytical formula for a sufficient diffusion time (note that the "threshold" time depends on Δx and the diffusion medium properties: the lower Δx or the higher D, the lower this threshold, cf. theorem 2). We have then proved that a macroscopic complex diffusion problem can be decomposed into a set of elementary diffusion processes controlled on an equally spaced grid which leads to a Gaussian probability Density Function. This decomposition illustrates M.S. El Naschie's idea that elementary processes of more complex systems are Gaussian [11].**5.3. 5.3.**
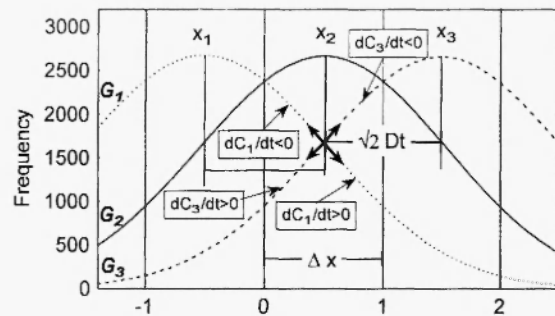

Fig. 4. Three adjacent cells x_1, x_2, x_3 of the space discretised grid $\Delta x = 1$ on which mesoscopic simulations are processed until the instability criterion is reached. Gaussian curves G1, G_2 and G_3 with standard deviation $\Delta x = \sqrt{2Dt} = 1$ ($D = 1, t = 1/2$, i.e. $\lambda = 1/2$) are centred on each cell.

Analysis of an elementary mesoscopic diffusion micro-state

Let us now consider three adjacent cells x_1, x_2, x_3 (Fig.4). Without lack of generality, we shall consider that $C(x_1, t_m, \Delta x) = C(x_2, t_m, \Delta x) = C(x_3, t_m, \Delta x)$ and $t_m = 0$. Supposing a long enough diffusion time, we get three Gaussian curves with the same area, centered on x_1, x_2, x_3 values and with a $\sqrt{2Dt}$ standard deviation. To obtain exactly the stability-instability threshold, from Eq.13 we

must have $\Psi(P) = 1$ which involves $\Delta x = \sqrt{2Dt}$ (if $\sqrt{2Dt} > \Delta x$ then the scheme is unstable). Fig.5 represents the three Gaussian curves at the instability threshold. Let us now analyze very precisely this critical density function. Each elementary cell diffuses on the adjacent intervals (a probability calculus shows that 24 % of the mass transfer is on adjacent cells). Let us now consider the x_2 interval. Concentration is the summation of all the Gaussian curves on these intervals. It is important to notice that the concentration in cell x_2 only results from the flux from cell x_1 and cell x_3. An important property is that, at the instability threshold, the inflexion points of the Gaussian curves G_1 and G_3 lie in the center of the interval x_2.

The following mathematical properties can be stated:

$$\begin{cases} \partial^2 C_{10}(x, \Delta x^2/2D, \Delta x)/\partial x^2 < 0 \\ \partial^2 C_{30}(x, \Delta x^2/2D, \Delta x)/\partial x^2 > 0, \\ \forall x \in [x_2 - \Delta x/2, x_2] \end{cases} \quad (28)$$

$$\begin{cases} \partial^2 C_{10}(x_2, \Delta x^2/2D, \Delta x)/\partial x^2 = 0 \\ \partial^2 C_{30}(x_2, \Delta x^2/2D, \Delta x)/\partial x^2 = 0 \end{cases}, \quad (29)$$

$$\begin{cases} \partial^2 C_{10}(x, \Delta x^2/2D, \Delta x)/\partial x^2 > 0 \\ \partial^2 C_{30}(x, \Delta x^2/2D, \Delta x)/\partial x^2 < 0. \\ \forall x \in [x_2, x_2 + \Delta x/2] \end{cases} \quad (30)$$

From Eq.2, $\partial^2 C_{i,j}(x,t,\Delta x)/\partial x^2 \propto \partial C_{i,j}(x,t,\Delta x)/\partial t$ then 50 % of the dx micro intervals ($dx \ll \Delta x$) of x_2 interval get a positive temporal gradient ($\partial C_{1,0}(x,t,\Delta x)/\partial t > 0$ and $\partial C_{3,0}(x,t,\Delta x)/\partial t > 0$), and 50% a negative gradient ($\partial C_{10}(x,t,\Delta x)/\partial t < 0$ and $C_{30}(x,t,\Delta x)/\partial t < 0$). After the stability threshold, more than 50% of micro cells get a negative gradient. This clearly means that the number of particles issued from adjacent cells x_1 and x_3 decreases with time (and so does the configuration entropy of the system x_2), which does not comply with the second principle of thermodynamics for a diffusive system... The mathematical criterion of stability for the explicit scheme is then physically related to the production of entropy: if the scheme is unstable then the production of

entropy on each discretised cell is negative ($\partial S_{n,m}(x,t,\Delta x)/\partial t < 0$). In chapter 7, we shall process a Monte Carlo simulation of diffusion to illustrate the mathematical tools of stability.

6. Numerical instability: an infringement of the second principle of thermodynamics.

In a monodimensional case, a PDE cell gets two adjacent PDE cells that will diffuse on this cell (see Fig.4).

We shall consider particles issued from the adjacent cells. At time origin, it was shown in the previous paragraph that no particle from the adjacent cells is present in the PDE cell. During the diffusion process, these particles will diffuse on the cell with respect to time. Let us now formulate the configuration of cells $x1$ or $x3$ in Fig.4. At the origin, entropy equals zero because no particle from the adjacent cells is present. Then entropy will increase thanks to diffusion. We shall now introduce the mathematical formalism of entropy evaluation. Based on the statistical thermodynamics, the PDE cell will be divided into k micro-systems of length δx, ($\Delta x = k\delta x, k \gg 1$) we call the 'Sub-PDE cells'. On each Sub-PDE cell, the probability of finding particles from the adjacent cells is evaluated and is of course time dependent. If the concentration in the PDE cell obeys the Gaussian hypothesis, the probability of having particles in an interval of length δx, ($\delta x \ll \Delta x$) located on x in the PDE-cell ($x \in [-\Delta x/2...\Delta x/2]$) is given by:

$$P(x,t,\Delta x,\delta x) = erf\left(\frac{\Delta x - x + \delta x}{\sqrt{4Dt}}\right) - erf\left(\frac{\Delta x - x}{\sqrt{4Dt}}\right).(31)$$

Then the entropy configuration on each Sub PDE-cell is given by:

$$\Delta S(x,t,\Delta x,\delta x) = -R\, P(x,t,\Delta x,\delta x)\log P(x,t,\Delta x,\delta x),$$
$$(32)$$

where R is the gas constant.

By means of entropy additivity, the entropy on any PDE-cell is then given by:

$$\Delta S(t, \Delta x, k) =$$

$$-R \sum_{i=-k/2+1}^{k/2} \left[\left[\left[erf\left(\frac{\Delta x\left(1 - \frac{i-1}{k}\right)}{\sqrt{4Dt}} \right) - erf\left(\frac{\Delta x\left(1 - \frac{i}{k}\right)}{\sqrt{4Dt}} \right) \right] \times \log\left[erf\left(\frac{\Delta x\left(1 - \frac{i-1}{k}\right)}{\sqrt{4Dt}} \right) - erf\left(\frac{\Delta x\left(1 - \frac{i}{k}\right)}{\sqrt{4Dt}} \right) \right] \right] \right]$$

$$(33)$$

and finally, the cell entropy is obtained when $\delta x \to 0$ meaning that $k \to \infty$:

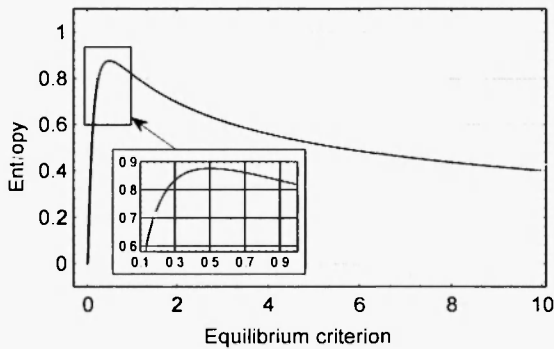$$\Delta S(t, \Delta x) = \lim_{k \to \infty} \Delta S(t, \Delta x, k) \qquad (34)$$

Fig. 5. Entropy calculation for the cell x_2 shown in Fig.4 by numerical estimation of Eq.33 for a configuration $k = 30$, $D = 1$, $\Delta x = 1$,

$t \in \{0, 0.001, 0.002, \cdots, 9.999, 10\}$ versus the values of stability criterion $\Delta t / \Delta x^2$. Entropy increases for the value of $\Delta t / \Delta x^2 = 0.5$ (graph zoom), and then entropy decreases.

Theorem 3:

$$\partial \Delta S(t, \Delta x) / \partial t > 0 \text{ if } \sqrt{2Dt} < \Delta x, t > 0, \qquad (35)$$

$$\partial \Delta S(t, \Delta x) / \partial t = 0 \text{ if } \sqrt{2Dt} = \Delta x, \qquad (36)$$

$$\partial \Delta S(t, \Delta x) / \partial t < 0 \text{ if } \sqrt{2Dt} > \Delta x. \qquad (37)$$

In instability cases, entropy will decrease in time which physically contradicts the second principle of thermodynamics (Table 2). We shall now estimate the entropy of the cell x_2 shown in Fig.5 by the numerical estimation of Eq. 33 for a particular configuration, $k = 30$, $D = 1$, $\Delta x = 1$, $t \in \{0, 0.001, 0.002, \cdots, 9.999, 10\}$.
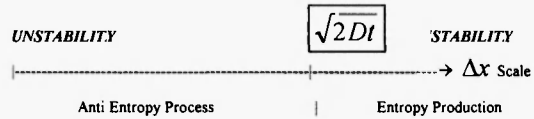

Table 2

Fig.6 represents the variation of the entropy of cell x_2 versus the values of the stability criterion $D \Delta t / \Delta x^2$. As can be observed, entropy increases up to $\Delta t / \Delta x^2 = 0.5$. Under this value the numerical scheme is stable, while over it the numerical scheme is unstable and entropy decreases. This is an illustration of the Prigogine and Brussels school which shows via stability
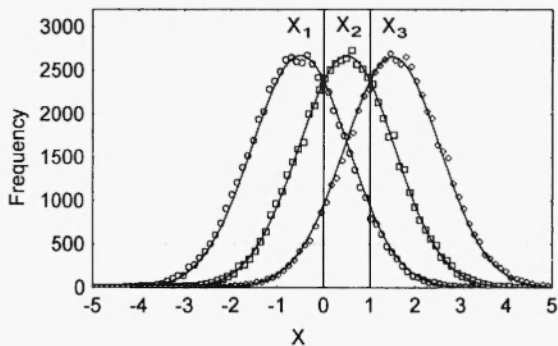

Fig. 6. Diffusion resulting from the three adjacent Cell-PDE modelled by a Brownian motion compared with the analytical solution under Gaussian hypothesis. n_v is the number of jumps of the particles, which corresponds to the time leading to the scheme instability (cf. Fig.5).

analysis that non-linear bifurcation can abruptly decrease local entropy [12]. In fact, for a given observation time Δt, if Δx decreases the probability of finding particles on Δx tends to decrease and then we tend to a time reversal that violates the time symmetry breaking induced by the second law of thermodynamics [13].

7. Monte Carlo simulation

The Brownian motion can also model the solution resulting from the PDE-cell. Physically speaking, p particles are uniformly randomly distributed on the interval $[x_n - \Delta x / 2, x_n + \Delta x / 2]$, divided into k subdivisions of length a at time

t_n ($\Delta x = k\,a$, $k \gg 1$). Then for each p particle, n_s jumps are processed on the left or on the right with a probability of one half. From the microscopic theory of diffusion, the diffusion coefficient is:

$$D = a^2 \Gamma / 2, \tag{38}$$

where Γ is the jump frequency of a particle from a micro-cell of length a to an adjacent micro cell.

The stability condition can then be expressed by including (10) into (38):

$$\frac{\Delta t}{(\Delta x)^2} \leq \frac{1}{a^2 \Gamma}. \tag{39}$$

Numerical application: $D = 1$, $k = 100$, $a = 10^{-2}$, $p = 100000$.

Then we get: $\Delta x = 1$, $n_s = \Gamma \Delta t$ (where n_s is the total number of jumps during time Δt) and the stability criterion (sc) becomes $n_s < (\Delta x / a)^2 = n_s^{sc} = 10000$. Firstly, we shall verify the convergence rate of theorem 1. We shall study the diffusion time effect between three adjacent cells for the values of $n_s \in \{1, 10, 100, 1000, 10000\}$. Fig.7 shows the concentration curves for these different evolution times and the theoretical Gaussian curves given by Eq.24 plotted for each concentration map. As can be observed, the convergence rate to the Gaussian curve is well adapted if $n_s > 1000$. As our theory induces the Gaussian approximation PDF for the case $n_s = n_s^{sc} = 10000$, then the Gaussian PDF is an adequate assumption.

We shall now study the case $n_s = n_s^{sc}$ for $k = 1000$, then $n_s^{sc} = 1000000$ more particularly. This simulation corresponds to a fine resolution of the diffusion problem on three adjacent cells at the instability threshold. Fig. 7 represents the theoretical solution (filled lines) under the Gaussian assumption (Eq.24) and the results from the Monte Carlo simulations. As can be observed, the Monte Carlo results converge towards the solution of the Gaussian approximation given by Eq.24 replacing the more complex Eq.23. This means that the Gaussian convergence claimed in theorem 1 is well accepted by our stability criterion and then
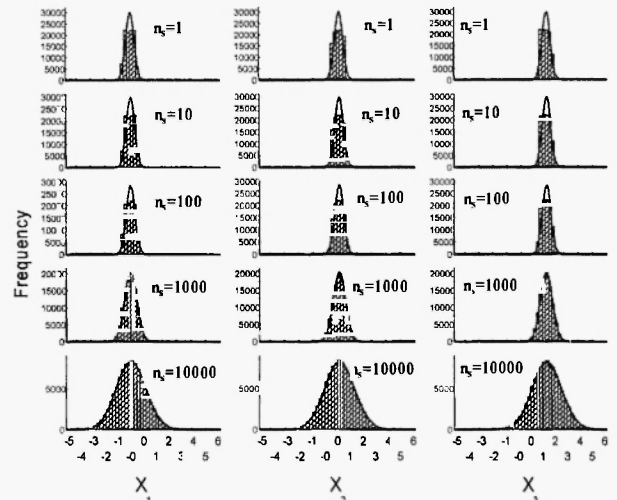

Fig. 7. Comparison of the solution of the diffusion on three adjacent Cell-PDE of length $\Delta x = 1000\,a$ modelled by a Brownian motion with the analytical solution under Gaussian hypotheses. The number of jumps $n_s^{sc} = 1000000$ of length a corresponds to the time leading to the scheme instability.

all our hypotheses are well posed. As a consequence, all our conclusions about stability and the relations with a physical interpretation speak for themselves in the practical case of finite simulation.

8. Conclusion

In this paper, we have shown that there exists a relation between the stability criterion that guarantees the convergence of the partial derivative equation to the solution and the physical interpretation at a mesoscopic scale under the size of discretisation. This interpretation is related to an infringement of the fundamental second principle of thermodynamics. Regarding the high number of stability studies found in the mathematical and physical bibliography, the stability threshold allows us to give a space and time definition onto which scales are well adapted to treat the physical problems at a mesoscopic scale. These criteria are pertinent to choose discretised time and space during a Monte Carlo simulation. The stability criterion gives a numerical evaluation of the threshold between mesoscopic and microscopic simulations. To build this theory,

an original mathematical tool was constructed: we have shown that complex macroscopic problems can be treated as sets of mesoscopic problems that can be solved analytically. This approach consists in choosing an adequate model for the physical phenomenon on the elementary cells to solve the physical problem in its integrity. We think that each element of discretisation must have some physical properties rather than mathematical asymptotic properties to solve physical differential problems. On the other hand it is in total agreement with Hadamard Conference (Zürich, 1917 cited in [14]) which disagrees with the common idea that a non-analytical partial derivative equation can be replaced by an analytical function without any significant effect, proving that an approximation could significantly disturb the solution.

In our case we have studied a linear equation that in fact could not lead to chaos. However we have shown that its discretisation scheme could lead to a chaotic (unstable) solution if discretization do not respect some physical considerations. This clearly means that diffusion equation, which leads to the differential equation, has lost a part of chaos due to asymptotic mathematical considerations. On the contrary, the diffusion map that we have proved to be physically realistic is highly non linear. From the information contained in these non linearity's, a space-time relation was stated proving that non linearity allows us to explore the deep properties of diffusion : *"If everything were linear, nothing would influence nothing"*, Einstein to Schrödinger (Cited in [13] with Author's comments about non linearity's effects in the space-time description).

We have only dealt with diffusion in a one-dimension space. We have studied the bi and three-dimensional cases and all results are confirmed. By applying our space-compactification principle [15, 16], we have found the same results using an isomorphism between concentration and Informions. These results, in agreement with Penrose's views on the computability of complex system [17-18], will be tackled in another paper.

References

1. Dautray R, Lions JL. *Analyse mathématique et Calcul numérique. Modèle physique*, Vol.1. Paris:Masson;1987.
2. Dautray R, Lions JL. *Analyse mathématique et Calcul numérique; Evolution, Fourrier, Laplace*, Vol.7. Paris:Masson;1992.
3. Dautray R, Lions JL. *Analyse mathématique et Calcul numérique; Numérique, transport* Vol.9. Paris:Masson; 1992.
4. Forsythe GE, Wasow WR. *Finite difference methods for partial differential equations*. New York:Wiley & sons;1960.
5. Peitgen HO, Jürgens H, Saupe D. *Chaos and Fractals New Frontiers of Science*. Berlin: Springer Verlag;1992.
6. Adda Y, Philibert J. *La diffusion dans les solides,* Tome II. Paris:Bibliotheque des Sciences et Techniques Nucléaires;1966.
7. Einstein A. *Investigation on the Theory of Brownian Motion.* New-York: Dover Pub.; 1956.
8. Bruhat G. *Thermodynamique*. Paris: Masson; 1962.
9. El Naschie M. S. Remarks on superstrings, fractal gravity, Wagasawa's diffusion and Cantorian Spacetime. *Chaos Solitons & Fractals* 1997;8:1873-86.
10. Stewart I. *Does God play dice? The new Mathematics of Chaos.* London: Penguin Books;1997
11. El Naschie M S. Branching polymer and the fractal Cantorian Space. *Chaos Solitons & Fractals* 1998;9:135-41.
12. Prigogine I. *From being to becoming.* New-York: Freeman;1980.
13. El Naschie M S. Time symmetry breaking, duality and Cantorian space-time. *Chaos Solitons & Fractals* 1996;7;4:499-518.
14. Gray J. *Le Défi de Hilbert.* France: Dunod; 2003.
15. Bigerelle M., lost A. Characterisation of the

diffusion states by data compression *Computational Material Science*, 2002;24; 133-8.

16. Bigerelle M., Iost A. Structure coarsening, entropy and compressed space Dimension, *Chaos, Solitons and Fractals*, 2003;18;665-79.

17. Penrose R. *Shadows of the Mind: a search for the missing science of consciousness.* Oxford: Oxford University Press;1996.

18. Penrose R. *The emperors's new mind.* Oxford: Oxford University Press;1999.